JJMIE

Volume 14, Number 4, December. 2020
ISSN 1995-6665
Pages 413 - 422

Jordan Journal of Mechanical and Industrial Engineering

Adaptive Disturbance Estimation and Compensation for Delta Robots

Iyad Hashlamon

Mechanical Engineering Department, Palestine Polytechnic University, Hebron, Palestine

Received March 14 2020 *Accepted November 22 2020*

Abstract

This paper introduces an adaptive disturbance estimation and compensation approach for delta parallel robots using three methods. The first method is based on the adaptive Kalman filter (AKF), the second method uses the Low pass filtered robot dynamic model (LFDM) while the third method is acceleration measurement based (AMB) method which utilizes the measured moving platform acceleration directly into the robot dynamical model. The considered disturbance is joint friction, uncertainty and unmodeled dynamics, their effects are represented as lumped disturbance torque vector. The estimation performance is evaluated using the mean square error (MSE) as a performance measure. To control the robot, the nonlinear robot model is linearized using feedback linearization through the estimated disturbance which is adaptively scaled using an adaptive tuning gain to overcome the limitations of the transient response of the estimated disturbance. The tuning is governed by a simple developed sliding surface depending on the error between the desired and actual joint angles. The tuned disturbance is added directly to the classical proportional–derivative (PD) controller output control signal for disturbance compensation and trajectory tracking. Based on the results, a comparison among the three methods is studied. The comparison shows that the AKF method is the most accurate that tracks the desired trajectory in the presence of disturbance and noise. The other methods are not recommended.

Keywords: Delta robot, adaptive Kalman filter, disturbance estimation, adaptive control;

1. Introduction

Parallel manipulator usage has been increased dramatically in industrial applications and attracted the academicians to conduct researches on design and control of these robots. Comparing this type of robots with serial robots, they have advantages in terms of light weight, high accuracy and repeatability, high stiffness, easy inverse kinematics computing, force distribution and short cycle times. Therefore, this type of robots is used in many applications that require high speed and acceleration, repeated work and accuracy such as: pick and place [1, 2], intelligent sorting systems [2, 3], 3D printing [4], food manufacturing systems [5], hybrid robot interaction [6] and many others [7, 8]. However, compared with serial robots, the computation of parallel robots forward kinematics is complicated and the dynamic model is challenging which complicates the implementation of some control algorithms such as inverse dynamic control and classical Proportional- integral derivative (PID) controllers [9]. More precisely, the dynamical model of the three degrees of freedom DoF Delta robot is composed of three dynamic nonlinear equations with three restriction equations.

Several classical control approaches were applied to match the desired performance and trajectory tracking [10-14]. The computed torque controllers require the full robot dynamic model. The unmodeled dynamics, joint friction, disturbances and model uncertainty deteriorate the controller performance [15]. PD and PID controllers are used to control delta robots [16]. The design principle neglects the coupling effects, thus the response is affected by the disturbance due to the structure of the robot and requires improving the tracking errors for robust and smooth response [17]. Joint friction has significant importance in terms of steady state error, limit cycles and poor dynamic response [18, 19]. Although friction has been represented by mathematical models [20-23], it is environment and load dependent. This increased the challenge to develop control approaches for joint friction compensation [24-28]. The structure of the Delta robot increases the difficulty to have an adaptive and a robust response. This paper will consider the unmodeled nonlinear coupled dynamics, model uncertainty and joint friction as lumped disturbance torque vector to be estimated and compensated.

Disturbance observers were used for disturbance estimation and compensation for robotic manipulators [29, 30]. These observers require knowledge of how to tune the observer gain. The active disturbance rejection control (ADRC) with linear disturbance observation and linear feedback control techniques are used for trajectory tracking tasks in parallel robots [9]. The estimation in the ADRC depends on the extended state observer [31]. This observer is regularly of high gain and requires a tuning process that avoids undesired high gain effects, such as peaking [32], instabilities or noisy estimations [33]. To overcome this limitation, an adaptive observer is used with a varying gain to form an adaptive active disturbance

* Corresponding author e-mail: iyad@ppu.edu.

rejection for robust trajectory tracking [34]. Many of the adaptive controllers of manipulators with dynamic uncertainty are Lyapunov -based [35, 36]. Lyapunov-based controllers focus more on stability and less on performance and require parameter tuning which is difficult. Recent nonlinear PD with sliding mode control was reported in [37]. However, sliding mode controller's major problem is chattering. The research on adaptive control of delta robot is still ongoing [38] to restrain model uncertainties problems. For a detailed comparison refer to [39].

This paper introduces an online adaptive disturbance estimation and compensation using three methods and compares among them. The first estimation method uses the adaptive Kalman filter AKF [40, 41] to estimate this disturbance. The structure of the AKF is recursive and considers the noise due to uncertainty and measurement noise and projects their effect on the filter gain. This gain is tuned adaptively depending on the estimation error. This filter is adaptive, i.e. it is unnecessary to know the statistics of the noise since it has two tuned updating rules for the noise covariance according to the estimation performance. The second method adopts the filtered dynamic model approach. The dynamic model of the robot contains the joint angular acceleration which is unmeasured or hard to be measured directly. This challenge is solved by filtering the dynamic model of the robot. The result of this method is a filtered version of the disturbance. This method is called low-pass filtered dynamic model LFDM. The third method is acceleration measurement based method AMB. This method assumes the availability of a three axes-accelerometer attached to the moving platform of the robot to measure its acceleration, then this measured acceleration is utilized in the robot model to estimate the disturbance.

The estimated disturbance will have transient response and overshoot. This will reduce the tracking performance of the controller. Therefore, to overcome this transient response, namely the overshoot, the estimated disturbance is adaptively tuned. A simple adaptive tuning gain surface is developed depending on the error between the actual and desired joint angles. This gain scales the estimated disturbance adaptively. In the steady state, the tuning gain effectiveness is decreased dramatically i.e. has a value of one or close to one. The tuned disturbance is added to the control signal of the classical PD controller to study the tracking trajectory performance. The proposed control approach shows that the adaptive disturbance estimation using AKF along with the PD controller result in smooth tracking of the desired trajectory.

The rest of the paper is organized as follows: Section 2 introduces the mathematical modeling of robot model, the problem statement is in section 3. Section 4 shows the disturbance estimation methods, Section 5 shows the control approach and Section 6 discusses the results. The paper is concluded in Section 7.

2. Mathematical modeling of the 3-DoF Delta robot

The Delta robot considered here is a 3- DoF robot which consists of three closed-loop kinematic chains, each chain represents parallelogram to ensure the constant orientation between the fixed platform and the moving platform in the task space as in Figure 1. The delta robot is equipped with three identical actuators fixed on the fixed platform which has the Newtonian frame *O*. The radius of the fixed platform is *f*. The moving platform has radius *r* with a frame E parallel to *O*. The parameters of the robot are listed in Table 1.

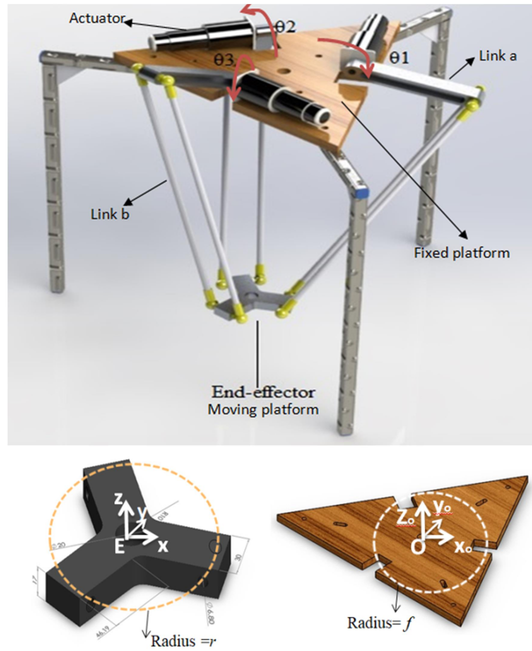

Figure 1. Delta robot

Table 1. Robot parameters

Description	Symbol	Unit
Length of link a	L_a	m
Length of link b	L_b	m
Radius of the fixed platform	f	m
Radius of the moving platform	r	m
Mass of link a	m_a	Kg
Mass of link b	m_b	Kg
Mass of the moving platform	m_p	Kg
Gravity acceleration	g	9.8 m/s^2
Elbow mass	m_e	Kg
Actuator inertia	$\mathbf{I}_m$	Kg.m^2
Gear ratio constant	k_G	-

The Delta robot dynamic model is described by a set of differential equations as

$$M(\boldsymbol{\theta})\ddot{\boldsymbol{\theta}} + C(\boldsymbol{\theta},\dot{\boldsymbol{\theta}})\dot{\boldsymbol{\theta}} + G(\boldsymbol{\theta}) + \boldsymbol{\tau}_{\mathbf{F}} = \boldsymbol{\tau} \ , \quad (1)$$

where $\boldsymbol{\theta} = [\theta_1 \quad \theta_2 \quad \theta_3]^T \in \mathbb{R}^3$ is the set of actuated joint vector. $\boldsymbol{\theta}$ is measured using joint encoders attached to the joint actuators. $M \in \mathbb{R}^{3\times3}$ is the positive definite inertia matrix, $C(\boldsymbol{\theta},\dot{\boldsymbol{\theta}})\dot{\boldsymbol{\theta}} \in \mathbb{R}^3$ vector represents the Coriolis and centrifugal torques, $G(\boldsymbol{\theta}) \in \mathbb{R}^3$ contains the gravitational terms acting on the robot. $\boldsymbol{\tau}_{\mathbf{F}} \in \mathbb{R}^3$ is the joint frictional vector and $\boldsymbol{\tau} \in \mathbb{R}^3$ is the generalized joint control vector. Also, the above terms include the moving plate position $\mathbf{p} \equiv \begin{bmatrix} p_x & p_y & p_z \end{bmatrix}^T$ in $\mathbb{R}^3$, the position vector starts from the origin of the frame O to the origin of the frame E. Then, the matrices M, C and G are given as follow [42]

$$M = \left(m_p + m_b\right) J^T J + \left(k_G^2 \mathbf{I}_m + L_a^2 \left(\frac{m_a}{3} + m_e + \frac{2}{3} m_b\right)\right) I_3$$

$$, C = J^T \left(m_p + m_b\right) \dot{J},$$

where I_q is the identity matrix of size q, J and $\dot{J}$ are the Jacobian and its time derivative respectively.

$$G(\theta) = \left[-J^T \left(m_p + m_b\right) \begin{bmatrix} 0 \\ 0 \\ -g \end{bmatrix} - \gamma m g \begin{bmatrix} \cos\theta_1 \\ \cos\theta_2 \\ \cos\theta_3 \end{bmatrix} \right],$$

where $m = m_a + m_e + \frac{2}{3} m_b$ and $\gamma = \dfrac{\frac{1}{2} m_a + m_e + \frac{2}{3} m_b}{m} L_a$

Link a_1 in chain one is rotated an angle of zero around the z_o axis in frame O, link a_2 in chain two is rotated an angle of 120^o and link a_3 in chain three is rotated an angle of 240^o. The Jacobian J is found by finding a closed loop position vector for each of the three chains and mapping the joint space variables to the Cartesian space variables. Since the length of link b is constant, this leads to three constraint equations.

3. Problem statement

In the ideal case where there is no external disturbance, the joint friction and the dynamic model are known, feedback linearization with PD controller will achieve the desired transient and steady state response for a manipulator by using simple linear pole placement techniques [39]. Unfortunately, in real systems disturbances and unmodeled dynamics exist. Further, the system parameters are not often precisely known. This paper considers the disturbance source from the uncertainty in the dynamic model inertia matrix $M(\boldsymbol{\theta})$, $C(\boldsymbol{\theta}, \dot{\boldsymbol{\theta}})$, $G(\boldsymbol{\theta})$ and $\boldsymbol{\tau}_{\mathbf{F}}$. That means, it is assumed that the inertia matrix $M(\boldsymbol{\theta})$ consists of two matrices; the constant diagonal matrix that represents the inertia of the robot upper links with the motor inertia $\mathbf{I}$ and the uncertainty in the inertia matrix $\tilde{M}(\boldsymbol{\theta})$, i.e. $M(\boldsymbol{\theta}) = \mathbf{I} + \tilde{M}(\boldsymbol{\theta})$. In addition, call the terms with uncertainty part as lumped nonlinear disturbance $\boldsymbol{\zeta}$, then Eq (1) can be rewritten as

$$\mathbf{I}\ddot{\boldsymbol{\theta}} + \boldsymbol{\zeta} = \boldsymbol{\tau}, \tag{2}$$

where $\boldsymbol{\zeta}$ is given by

$$\boldsymbol{\zeta} = C(\boldsymbol{\theta}, \dot{\boldsymbol{\theta}})\dot{\boldsymbol{\theta}} + G(\boldsymbol{\theta}) + \boldsymbol{\tau}_{\mathbf{F}} + \tilde{M}(\boldsymbol{\theta})\ddot{\boldsymbol{\theta}}, \tag{3}$$

and must be estimated and used in the control law for disturbance compensation.

Equation (2) can be written in state space form by choosing the actuated motors angular displacements and velocities as states:

$$\mathbf{x} \equiv \begin{bmatrix} x_1 & \cdots & x_6 \end{bmatrix}^T = \begin{bmatrix} \theta_1 & \theta_2 & \theta_3 & \dot{\theta}_1 & \dot{\theta}_2 & \dot{\theta}_3 \end{bmatrix}^T$$

$$\dot{\mathbf{x}} = \underbrace{\begin{bmatrix} 0_{3\times3} & I_3 \\ 0_{3\times3} & 0_{3\times3} \end{bmatrix}}_{A} \mathbf{x} + \underbrace{\begin{bmatrix} 0_{3\times3} \\ \mathbf{I}^{-1} \end{bmatrix}}_{B} \mathbf{u} + \underbrace{\begin{bmatrix} 0_{3\times3} \\ -\mathbf{I}^{-1} \end{bmatrix}}_{F_d} \boldsymbol{\zeta}, \tag{4}$$

where $\mathbf{x}$ is the state vector, $0_{q\times\beta}$ is zero matrix of size $q \times \beta$ and $\mathbf{u} = \boldsymbol{\tau}$. The measurement vector can be represented as

$$y = \underbrace{\begin{bmatrix} I_3 & 0_{3\times3} \end{bmatrix}}_{H} \mathbf{x} \tag{5}$$

4. Disturbance estimation

It is possible to estimate the lumped disturbance vector using several methods: AKF, LFDM and AMB methods. The estimation depends on the knowledge of the applied control torque at the joint. The model in Eq (2) is rewritten in other representations suitable for each estimation method.

AKF method

The AKF is an adaptive observer for linear systems, it is used to estimate the disturbance by augmenting the disturbance with the states as an extended state, accordingly, Eq (4) is rewritten in the form

$$\begin{bmatrix} \dot{\mathbf{x}} \\ \dot{\boldsymbol{\zeta}} \end{bmatrix} = \begin{bmatrix} A & F_d \\ 0_{3\times6} & 0_{3\times3} \end{bmatrix} \begin{bmatrix} \mathbf{x} \\ \boldsymbol{\zeta} \end{bmatrix} + \begin{bmatrix} B \\ 0_{3\times3} \end{bmatrix} \mathbf{u}, \tag{6}$$

The measurement vector consists of the active joint angles that are measured using joint encoders attached to the joint actuators. In addition to that, differentiating the angular position numerically using backward Euler formula gives valuable information. Hence $\dot{\boldsymbol{\theta}}$ is considered as pseudo measured. Discretizing Eq (6) using backward Euler formula yields

$$\begin{gathered} \begin{bmatrix} \mathbf{x}(k) \\ \boldsymbol{\zeta}(k) \end{bmatrix} = A_d \begin{bmatrix} \mathbf{x}(k-1) \\ \boldsymbol{\zeta}(k-1) \end{bmatrix} + B_d u(k) + \upsilon(k-1) \\ z = H_{new} \begin{bmatrix} \mathbf{x}(k) \\ \boldsymbol{\zeta}(k) \end{bmatrix} + \nu(k) \end{gathered}, \tag{7}$$

where

$$A_d = \begin{bmatrix} I_3 & TI_3 & \mathbf{0}_{3\times3} \\ \mathbf{0}_{3\times3} & I_3 & -T\mathbf{I}^{-1} I_3 \\ \mathbf{0}_{3\times3} & \mathbf{0}_{3\times3} & I_3 \end{bmatrix}, B_d = \begin{bmatrix} \mathbf{0}_{3\times3} \\ T\mathbf{I}^{-1} \\ \mathbf{0}_{3\times3} \end{bmatrix}, \tag{8}$$

$H_{new} = \begin{bmatrix} I_6 & 0_{6\times3} \end{bmatrix}$ is the output matrix, T is the sampling time and k is the time index. $\upsilon \in \mathbb{R}^9$ and $\nu \in \mathbb{R}^6$ are the zero mean Gaussian process and measurement noises with covariance matrices Q and R respectively, i.e. $\upsilon \sim N(0, Q)$ and $\nu \sim N(0, R)$. The covariance matrices Q and R are unknown and have an important effect on Kalman filter estimates. If the given value of Q is much smaller than the true value, then the result is biased estimated states $\hat{\mathbf{x}}$ and $\hat{\zeta}$. On the other hand, if the given value of Q is much larger than the true value, then the estimated states $\hat{\mathbf{x}}$ and $\hat{\boldsymbol{\zeta}}$ will oscillate around the true value. The advantage of the AKF [40] is that it does not need the values of the noise covariance matrices, just initial values of them are required. Then by its recursive structure, it updates the covariance matrices based on the innovation e between the predicted states and the measured vector. This error is used to update and correct the predicted states through Kalman gain which takes into the consideration the uncertainty in the model through the covariance matrices. The output of this filter are the estimated states $\hat{\mathbf{x}}$ and $\hat{\zeta}$. The following assumptions are considered:

- **Assumption 1**: The process and measurement noises are assumed to be independent and mutually uncorrelated.
- **Assumption 2:** The inputs are considered to be piecewise constant over the sampling time interval *T*.

The AKF requires positive constants N_R and N_Q, initial values of matrices R_0 and Q_0, and an initial value of the estimation error covariance matrix P_0. The AKF algorithm is shown between Eqs (9) and (23) respectively.

Initial values $\bar{\varpi}_0, \bar{e}_0, \hat{x}_0, P_0, N_R, N_Q, Q_0 > 0,\ R_0 > 0$

$$\begin{bmatrix} \hat{\mathbf{x}}^-(k) \\ \hat{\zeta}^-(k) \end{bmatrix} = A_d \begin{bmatrix} \hat{\mathbf{x}}(k-1) \\ \hat{\zeta}(k-1) \end{bmatrix} + B_d\, u(k), \tag{9}$$

$$P^-(k) = A_d\, P(k-1)\, A_d^T + Q(k-1), \tag{10}$$

$$e(k) = z(k) - H_{new} \begin{bmatrix} \hat{\mathbf{x}}^-(k) \\ \hat{\zeta}^-(k) \end{bmatrix}, \tag{11}$$

$$\alpha_1 = \frac{N_R - 1}{N_R}, \alpha_2 = \frac{N_Q - 1}{N_Q}, \tag{12}$$

$$\bar{e}(k) = \alpha_1\, \bar{e}(k-1) + \frac{1}{N_R} e(k), \tag{13}$$

$$\begin{aligned} \Delta R(k) = &\frac{1}{N_R - 1}\left(e(k) - \bar{e}(k)\right)\left(e(k) - \bar{e}(k)\right)^T \\ &-\frac{1}{N_R}\left(H_{new}\, P^-\, H_{new}^T\right)_{(k)} \end{aligned} \tag{14}$$

$$R(k) = \alpha_1\, R(k-1) + \Delta R(k), \tag{15}$$

$$K(k) = P^-(k)\, H_{new}^T \left(H_{new}\, P^-(k)\, H_{new}^T + R(k)\right)^{-1}, \tag{16}$$

$$\begin{bmatrix} \hat{\mathbf{x}}(k) \\ \hat{\zeta}(k) \end{bmatrix} = \begin{bmatrix} \hat{\mathbf{x}}^-(k) \\ \hat{\zeta}^-(k) \end{bmatrix} + K(k)\, e(k), \tag{17}$$

$$P(k) = \left(I - K(k) H_{new}\right) P^-(k), \tag{18}$$

$$\hat{\omega}(k) = \begin{bmatrix} \hat{\mathbf{x}}(k) \\ \hat{\zeta}(k) \end{bmatrix} - \begin{bmatrix} \hat{\mathbf{x}}^-(k) \\ \hat{\zeta}^-(k) \end{bmatrix}, \tag{19}$$

$$\bar{\varpi}(k) = \alpha_2\, \bar{\varpi}(k-1) + \frac{1}{N_Q} \hat{\omega}(k), \tag{20}$$

$$\begin{aligned} \Delta Q(k) = &\frac{1}{N_Q}\left(P(k) - A_d\, P(k)\, A_d^T\right) \\ &+ \frac{1}{N_Q - 1}\left(\hat{\omega}(k) - \bar{\varpi}(k)\right)\left(\hat{\omega}(k) - \bar{\varpi}(k)\right)^T \end{aligned}, \tag{21}$$

$$Q(k) = \alpha_2\, Q(k-1) + \Delta Q(k), \tag{22}$$

$$\begin{aligned} Q(k-1) &= \left| diag\left(Q(k)\right)\right|, \\ R(k-1) &= \left| diag\left(R(k)\right)\right| \end{aligned}. \tag{23}$$

where $(.)^-$ and $(.)$ stand for the prior and posterior estimates, respectively. K is the Kalman gain. $z \in \mathbb{R}^6$ is the measurement vector and $\hat{\omega}$ is the state error.

Implementation note: for a noisy system, it is much better to give more weight to the previous known values $\left(R(k-1), Q(k-1)\right)$ than the current noisy reading, and this is achieved by selecting big N_R and/or N_Q. In the same context, small N_R and/or N_Q give more weight to the current reading $\left(\Delta R_k, \Delta Q_k\right)$ for less noisy readings.

Low pass filtered dynamic model method LFDM

The robot model in Eq (2) can be rewritten as

$$\boldsymbol{\zeta} = \boldsymbol{\tau} - \mathbf{I}\ddot{\boldsymbol{\theta}}, \tag{24}$$

The right hand-side of Eq (24) can be computed if the angular acceleration $\ddot{\boldsymbol{\theta}}$ is known. However, in most cases this acceleration is unmeasured. The filtered dynamic model [26, 43, 44] avoids the explicit calculation of this acceleration by filtering both sides of Eq (24) using a proper stable filter. For this 3-DoF robot, three first order filters with three constants σ_i for i=1,2,3 are used. The transfer function of each filter $\mathbb{Z}_i(s)$ and the corresponding impulse response $z_i(t)$ are written as

$$\mathbb{Z}_i(s) = \sigma_i \frac{1}{s + \sigma_i}, \tag{25}$$

and

$$z_i(t) = \ell^{-1}\left(\mathbb{Z}_i(s)\right) = \sigma_i e^{-\sigma_i t}, \tag{26}$$

respectively, where $\ell^{-1}(.)$ is the Laplace inverse transform and s refers to Laplace transform. Then the impulse response for the 3-DoF robot is

$$\mathbf{z}(t) = \begin{bmatrix} \sigma_1 e^{-\sigma_1 t} & 0 & 0 \\ 0 & \sigma_2 e^{-\sigma_2 t} & 0 \\ 0 & 0 & \sigma_3 e^{-\sigma_3 t} \end{bmatrix}. \tag{27}$$

Since the multiplication in the frequency domain is equivalent to the convolution in time domain, then the filtered version of Eq (24) is

$$\int_0^t \mathbf{z}(t-\tau)\zeta d\tau = \int_0^t \mathbf{z}(t-\tau)\boldsymbol{\tau} d\tau - \int_0^t \mathbf{z}(t-\tau)\mathbf{I}\ddot{\boldsymbol{\theta}} d\tau \tag{28}$$

Remembering that $\mathbf{I}$ is constant matrix, then $\dot{\mathbf{I}} = 0$. Further at time $t = 0$, the initial condition $\dot{\boldsymbol{\theta}}(0) = 0$ and the impulse response is the diagonal matrix

$\mathbf{z}(0)=\boldsymbol{\sigma}=diag(\sigma_1,\sigma_2,\sigma_3)$. Having that, the term $\int_0^t \mathbf{z}(t-\tau)\mathbf{I}\ddot{\boldsymbol{\theta}}d\tau$ will be

$$\int_0^t \mathbf{z}(t-\tau)\mathbf{I}\ddot{\boldsymbol{\theta}}d\tau=\boldsymbol{\sigma}\mathbf{I}\dot{\boldsymbol{\theta}}-\int_0^t \dot{\mathbf{z}}(t-\tau)\mathbf{I}\dot{\boldsymbol{\theta}}d\tau \quad (29)$$

where $\dot{\mathbf{z}}$ is the derivative of the filter response

$$\dot{\mathbf{z}}(t)=-diag\left(\sigma_1^2e^{-\sigma_1 t},\sigma_2^2e^{-\sigma_2 t},\sigma_3^2e^{-\sigma_3 t}\right), \quad (30)$$

or in Laplace domain

$$\ell\{\dot{z}_i(t)\}=\ell\{-\sigma_i^2e^{-\sigma_i t}\}=-\sigma_i^2\frac{1}{s+\sigma_i}.$$

Using the above equations, the filtered model is

$$\int_0^t \mathbf{z}(t-\tau)\boldsymbol{\zeta}d\tau=-\boldsymbol{\sigma}\mathbf{I}\dot{\boldsymbol{\theta}}+\int_0^t \mathbf{z}(t-\tau)(\boldsymbol{\tau})d\tau+\int_0^t \dot{\mathbf{z}}(t-\tau)\mathbf{I}\dot{\boldsymbol{\theta}}d\tau \quad (31)$$

The left hand side of Eq (31) is the resulted filtered version of the disturbance using the filter in Eq (25). The right hand side is filtered using either Eq (25) or Eq (30). The cut-off frequency of the first order filter depends on the highest basic frequency in the measurements. It is user defined.

Acceleration measurement-based estimation method AMB

This method considers the existence of a three axes-accelerometer at the moving platform. Thus, the acceleration vector $\mathbf{a}\equiv\ddot{\mathbf{p}}=\dot{\mathbf{v}}$ is considered being measured and can be expressed as

$$\mathbf{a}=J\ddot{\boldsymbol{\theta}}+\dot{J}\dot{\boldsymbol{\theta}}. \quad (32)$$

Then the robot model in Eq (2) along with Eq (32) lead to estimate the disturbance as

$$\boldsymbol{\zeta}=\boldsymbol{\tau}-\mathbf{I}J^{-1}\left(\mathbf{a}-\dot{J}\dot{\boldsymbol{\theta}}\right). \quad (33)$$

This method depends directly on the measured angular velocity.

5. Control approach

The controller has two parts. The first part of the presented control architecture is a stabilizing and robust tracking mechanism using a PD controller that is designed to track the reference trajectory. The second part is the adaptive disturbance compensation.

PD controller

In the ideal case, consider that the estimated lumped disturbance vector $\hat{\boldsymbol{\zeta}}$ converged to the true value of $\boldsymbol{\zeta}$, i.e. $\boldsymbol{\zeta}-\hat{\boldsymbol{\zeta}}\to 0$. Then for the model Eq (2), after some mathematical manipulation, the error dynamics is given as

$$\ddot{\mathbf{e}}+k_d\dot{\mathbf{e}}+k_p\mathbf{e}=0 \quad (34)$$

Where $\mathbf{e}=\boldsymbol{\theta}-\boldsymbol{\theta}_d$, $\boldsymbol{\theta}_d$ is the desired trajectory, k_p and k_d are the positive gains of the PD controller which can be determined using pole placement techniques.

Adaptive disturbance compensation

The estimated disturbance is used to achieve the feedback linearization adaptively so that linear controllers are applied. The estimated disturbance is added directly to the PD controller output. However, in the transient response, the estimated disturbance $\hat{\boldsymbol{\zeta}}$ suffers from the overshoot which affects the robot response adversely. Therefore, a tuning gain $\lambda=diag(\lambda_1,\lambda_2,\lambda_3)$ is introduced to scale $\hat{\boldsymbol{\zeta}}$ adaptively. The gain range is $\lambda\in(0,1]$.

Define the maximum value of the error $\mathbf{e}$ as $\mathbf{e}_\mathrm{m}\equiv\begin{bmatrix}\mathbf{e}_{\mathrm{m}_1} & \mathbf{e}_{\mathrm{m}_2} & \mathbf{e}_{\mathrm{m}_3}\end{bmatrix}^T$ and the positive constant $k_t\equiv\begin{bmatrix}k_{t_1} & k_{t_2} & k_{t_3}\end{bmatrix}^T$. Both $\mathbf{e}_\mathrm{m}$ and k_t are user defined. For simplicity, only the scalar case is considered. It is desired that the gain λ scales $\hat{\boldsymbol{\zeta}}$ in the transient response when is has the overshoot. While at the steady state, the value of λ is one or close to one. The design of λ is based on $\mathbf{e}$, when the error $\mathbf{e}$ is big, then majority of the effort is given to the PD controller; this is accomplished by decreasing the gain λ. On the other hand, when the error $\mathbf{e}$ decreases, λ increases to its maximum value of unity. As shown in Figure **2**, when the error $\mathbf{e}\to\mathbf{e}_\mathrm{m}$ specially at the initial run of the estimator, λ value will be k_t i.e. $\lambda=k_t$. Once the error converges, λ value will be close to one, i.e. $\lambda\approx 1$, hence the same estimated disturbance $\hat{\boldsymbol{\zeta}}$ is added to the PD controller output. The mathematical representation of the tuning gain for the three joints is given by

$$\lambda=\begin{bmatrix}-\frac{1-k_{t_1}}{\mathbf{e}_{\mathrm{m}_1}}|\mathbf{e}_1|+1 & 0 & 0\\ 0 & -\frac{1-k_{t_2}}{\mathbf{e}_{\mathrm{m}_2}}|\mathbf{e}_2|+1 & 0\\ 0 & 0 & -\frac{1-k_{t_3}}{\mathbf{e}_{\mathrm{m}_3}}|\mathbf{e}_3|+1\end{bmatrix}$$

(35)

and the corresponding tuned disturbance is $\lambda\hat{\boldsymbol{\zeta}}$. The overall control approach is shown in Figure 3.

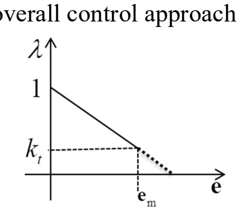

Figure 2. Disturbance tuning gain

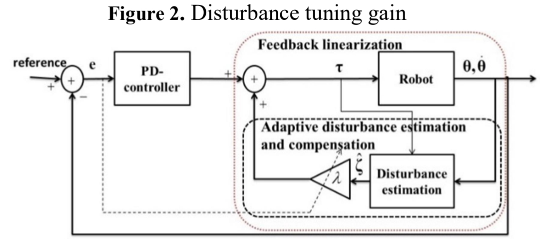

Figure 3. Adaptive feedback linearization and control of delta robot

6. Experimental Simulation Results

To evaluate the estimation and tracking performance, the true joint friction is required. However, since it is difficult to measure the friction, MATLAB environment is used as an experimental platform to carry out simulations on the robot model. The experiments are carried on 3-DoF delta robot model as shown in Figure 1. The values of the delta robot parameters are given in Table 2, for more details on the robot model refer to [45]. To be more realistic, Gaussian noise was added to both the measured acceleration and the pseudo measured angular velocity. This noise was generated using MATLAB Simulink Gaussian noise generator with zero mean and variance 0.001. The sampling time of this simulation T=0.001s. The original nonlinear model of the robot is used throughout the simulation.

The true joint friction is generated using the nonlinear model [23].

$$\boldsymbol{\tau}_{\mathbf{F}} = \gamma_1\left(\tanh\left(\gamma_2\dot{\boldsymbol{\theta}}\right) - \tanh\left(\gamma_3\dot{\boldsymbol{\theta}}\right)\right) + \gamma_4\tanh\left(\gamma_5\dot{\boldsymbol{\theta}}\right) + \gamma_6\dot{\boldsymbol{\theta}} \quad (36)$$

where $\gamma_i, i = 1,\cdots,6$ are positive constants and the static coefficient of friction can be approximated by $\gamma_1 + \gamma_4$. The stribeck effect is represented by $\left(\tanh\left(\gamma_2\dot{\boldsymbol{\theta}}\right) - \tanh\left(\gamma_3\dot{\boldsymbol{\theta}}\right)\right)$, $\gamma_4\tanh\left(\gamma_5\dot{\boldsymbol{\theta}}\right)$ and $\gamma_6\dot{\boldsymbol{\theta}}$ represent the coulomb friction and the viscous dissipation respectively. Each of the active joints has the same adopted friction model. The values of the parameters $\gamma_i, i = 1,\cdots,6$ are listed in Table 3

Table 2. The values of the Delta robot parameters

Parameter	Value
f	0.1 m
r	0.055 m
L_a	0.18 m
L_b	0.435 m
Mass of moving platform	0.196 kg
Mass of elbow	0.024 kg
Mass of link b	0.055 kg
Mass of link a	0.190 kg
Motor inertia	81.6×10^{-3};
Motor gear ratio constant	0.01

Before the estimation takes place, a traditional PD controller is used with the transfer function

$$PD(s) = k_p + k_d N\frac{s}{s+N} \;, \quad (37)$$

here $k_p = 25I_3$ $k_d = I_3$ and N=100, these values were selected to obtain the best possible trajectory tracking response without disturbance compensation as depicted in

Figure 4 which shows the error between the desired and the actual trajectories.

Table 3. Friction model parameters for each joint

Friction model constants	Joint 1	Joint 2	Joint 3
γ_1	0.7	0.6	5
γ_2	10	10	10
γ_3	10	10	10
γ_4	0.6	0.5	0.4
γ_5	50	100	10
γ_6	0.9	0.9	0.9

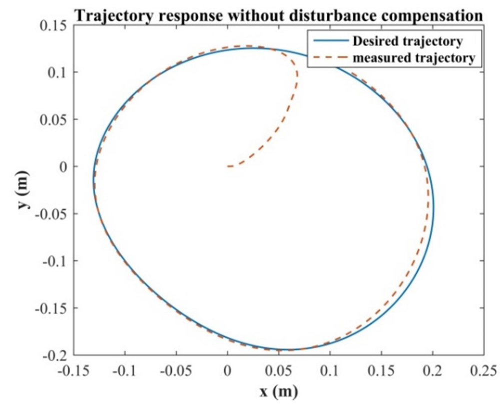

Figure 4. Trajectory response without disturbance compensation.

6.1. Disturbance Estimation Performance

The estimation is carried out simultaneously for all the active joints using the three methods. The AKF is recursive-based estimation and requires initializations which are listed in Table 4. The error initial values were set to zero. The state covariance errors were set to 100 since the error between the estimated value and the true value is large at the beginning. The values of N_R and N_Q are set to be equal which is not necessary for all systems, they can have different values. The LFDM requires the filter constant σ which is selected to be 5 for all joints. Low values of the filter cut off frequency will deteriorate the dynamics of the estimated disturbance.

In order to evaluate the estimation performance, the estimated results at this section were obtained without disturbance compensation. For the simulation purposes, the acceleration of the moving platform is computed using Eq (32).

Table 4. AKF parameters and initializations

Parameter	Value	Parameter	Value
$R(0)$	$0.1I_6$	$\overline{e}(0)$	$\mathbf{0}_{6\times1}$
$Q(0)$	$0.001I_9$		10^6
$P(0)$	$100I_9$	N_Q	10^6
$\hat{\mathbf{x}}(0)$	$\mathbf{0}_{6\times1}$	$\mathbf{u}(0)$	$\mathbf{0}_{3\times1}$
$\hat{\zeta}(0)$	$\mathbf{0}_{3\times1}$	$\overline{\varpi}(0)$	$\mathbf{0}_{9\times1}$

The estimated disturbance vector $\hat{\zeta}$ at the three active joints using the three methods is depicted in Figure 5. The estimated disturbance using the AMB method has very high overshoot, and it converges to the true value faster than the LFDM. On the other hand, the AKF tracks the true value and has the best response among the three methods in terms of overshoot, convergence speed and tracking. Further, the AKF considers the noise either in the process or in the measurement through the matrices Q and R and reflects them on the filter gain. At the same time, it tunes the filter gain adaptively according to the estimation performance.

The AMB method suffers from very high overshoot. Further, it is very sensitive to the noise which may limit its use. As a performance measure, the mean square error (MSE) is used. The MSE is given by

$$MSE(j) = \frac{1}{n}\sum_{i=1}^{n}\left(\zeta(j) - \hat{\zeta}(j)\right)^2 , \tag{38}$$

where n is the number of measurements and j=1,2,3 is the active joint index . Table 5 shows the MSE of $\hat{\zeta}$ for the three joints. Accordingly, the AKF has the best MSE, the AMB performance depends on the quality of the measurement.

In terms of implementation and requirements, the AMB does not require any constants or initializations, the LFDM requires the filter constant. On the other hand, the AKF requires several initializations which are easy to be initialized and then will be tuned adaptively according to the filter performance. In terms of noise considerations, only the AKF considers the noise through the process and measurement noise covariance matrices.

In terms of computational cost, the AKF has more cost than the other methods due to the algorithm structure. The LFDM has the lowest computational cost.

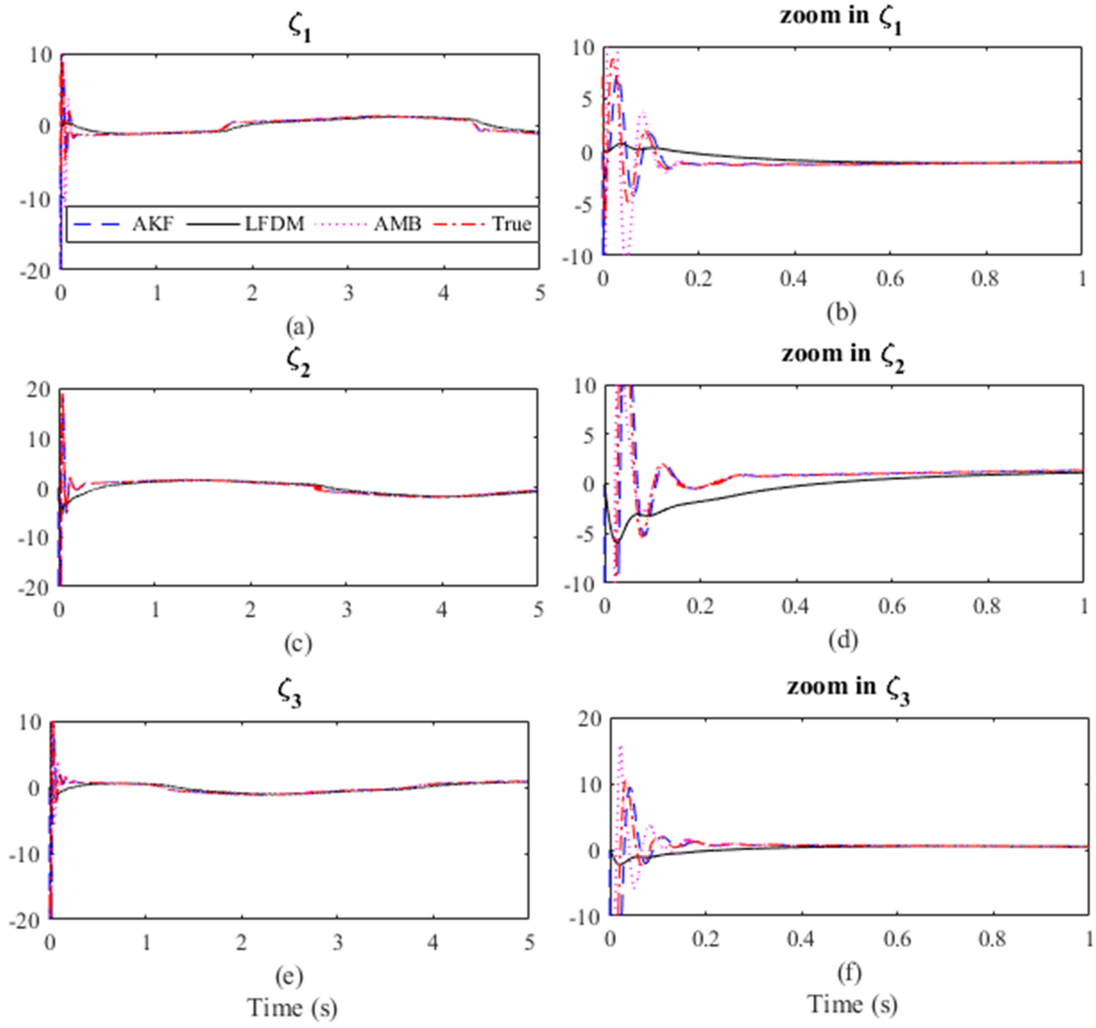

Figure 5. Estimated disturbance a) $\hat{\zeta}_1$, b) zoomed version of $\hat{\zeta}_1$, c) $\hat{\zeta}_2$, d) zoomed version of $\hat{\zeta}_2$ e) $\hat{\zeta}_3$ and f) zoomed version of $\hat{\zeta}_3$ using the three methods

Table 5. MSE of the estimated disturbance using the three methods

Joint	AKF	LFDM	AMB
Joint 1	0.0003	0.0004	0.0028
Joint 2	0.0028	0.0042	0.0042
Joint 3	0.0011	0.0034	0.0027

6.2. Disturbance compensation performance and discussion

The estimated disturbance $\hat{\zeta}$ is added directly to the control signal from the PD controller to form online disturbance estimation and compensation. Although the previous section shows the quality of the estimated disturbance, however, the transient estimation response affects the control law diversely. Therefore a tuning gain λ is added as in Figure 3. The response of disturbance compensation based on the AKF is depicted in Figure 6. The moving plate starts from its home position to track the desired trajectory with an overshoot. This response is expected according to the estimated disturbance discussed before. Also, it is expected that this method is much better than the other methods.

The gain λ values are plotted in Figure 7. $\mathbf{e}_{\mathrm{m}} = \begin{bmatrix}1 & 1 & 1\end{bmatrix}^T$ and $k_t = \begin{bmatrix}0.3 & 0.3 & 0.3\end{bmatrix}^T$ are considered. As clear the gain for $\hat{\zeta}_1$ starts with value of 0.87 in the period of the transient response of the estimated disturbance. This indicates that 87% of the estimated disturbance $\hat{\zeta}_1$ is passed to the control law. For $\hat{\zeta}_2$, it has more overshoot than $\hat{\zeta}_1$ using the same estimator AKF, this explains the reason of the value of the gain to be 0.38. Then the gain converges to be close to one i.e. the same estimated disturbance is used with the control law.

The LFDM method has steady state error under the same running conditions as shown in Figure 8. The tuned gain depicted in Figure 9 starts from a value of 0.35. This confirms the observation in Figure 5. As shown in Figure 5, the LFDM deteriorates the dynamics of the signal, this is confirmed in Figure 9 as the gain converges to one with less oscillations compared with AKF.

Lastly, the AMB method is not recommended according to Figure 10 and Figure 11.

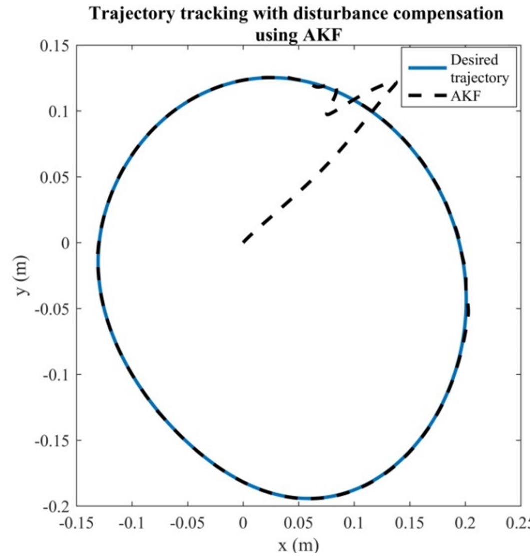

Figure 6. Trajectory tracking with disturbance compensation using AKF

7. Conclusion

The main contribution of this paper is to implement an adaptive estimation-control approach to satisfy a predefined performance with tuning few parameters. The Disturbance deteriorates the tracking performance of the delta robot. This paper studied three methods of disturbance estimation by considering the lumped disturbance vector. The AKF method is the most accurate and has a fast convergence. This method is adaptive by the nature of the AKF and supports the adaptive trajectory tracking. The required initializations are randomly selected, and the filter updates the results adaptively. This AKF method is applicable to robots in general and not only to delta robot. The other methods cause tracking errors and are not recommended. Further, to overcome the initial estimation dynamics challenge on the control system and to enhance the control flexibility, an adaptive controller is used with the disturbance to form the adaptive disturbance compensation. As a result, the PD controller can perform well to get the desired performance. The proposed controller gives better results in terms of steady-state error.

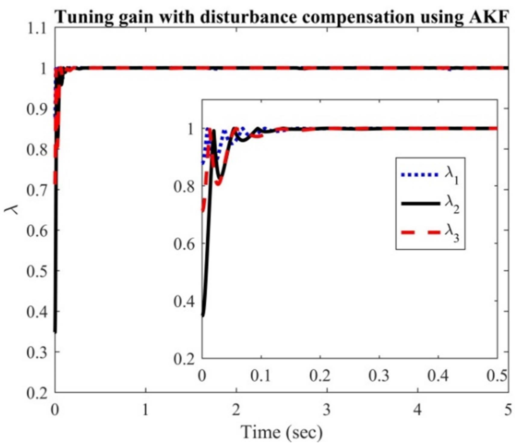

Figure 7. The tuning gain with disturbance compensation using AKF

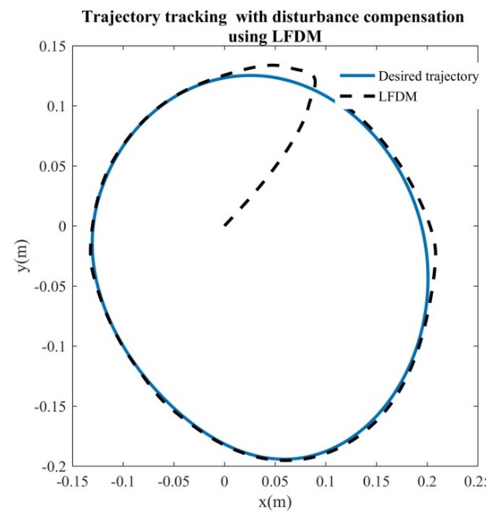

Figure 8. Trajectory tracking with disturbance compensation using LFDM

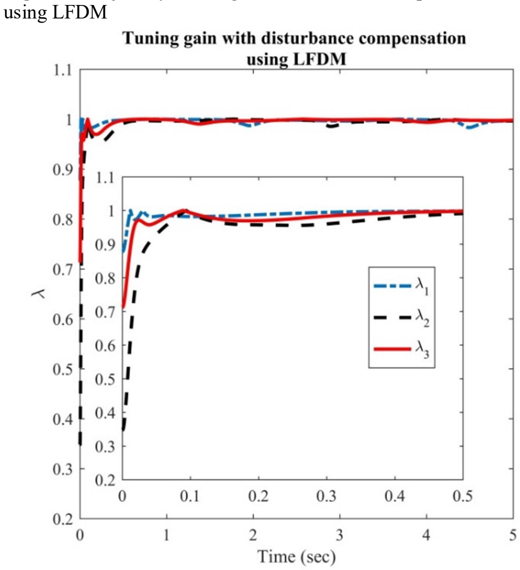

Figure 9. The tuning gain with disturbance compensation using LFDM

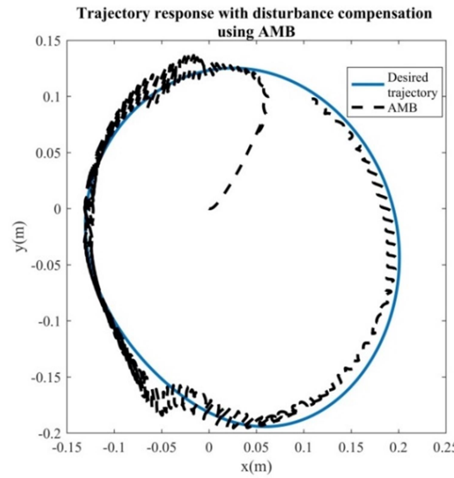

Figure 10. Trajectory response with disturbance compensation using AMB

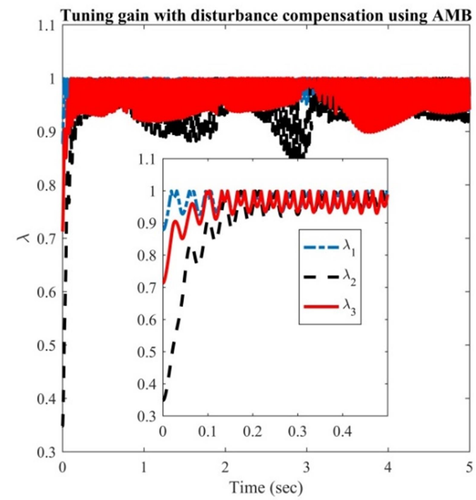

Figure 11. The tuning gain with disturbance compensation using AMB

References

[1] V. Nabat, M. de la O Rodriguez, O. Company, S. Krut, and F. Pierrot. "Par4: very high speed parallel robot for pick-and-place". IEEE/RSJ International Conference on intelligent robots and systems, 2005.

[2] T. Huang, J. Mei, Z. Li, X. Zhao, and D. G. Chetwynd, "A method for estimating servomotor parameters of a parallel robot for rapid pick-and-place operations". Journal of Mechanical Design, Vol. 127, No. 4, 2005, pp. 596-601.

[3] S. Wang, H. Lin, R. Gai, and Y. Sun. "An application of vision technology on intelligent sorting system by delta robot". IEEE 19th International Conference on e-Health Networking, Applications and Services (Healthcom), 2017.

[4] J. Pattavanitch and S. Panyaru, "Development of a new linear delta robot for the fused deposition modelling process". Journal of Research and Applications in Mechanical Engineering, Vol. 5, No. 1, 2017, pp. 42-54.

[5] Z. H. Khan, A. Khalid, and J. Iqbal, "Towards realizing robotic potential in future intelligent food manufacturing systems". Innovative food science & emerging technologies, Vol. 48, No. 2018, pp. 11-24.

[6] X. Zhang, R. Zhang, L. Chen, and X. Zhang. "Natural Gesture Control of a Delta Robot Using Leap Motion". Journal of Physics: Conference Series, 2019.

[7] D. Grajewski, F. Gorski, D. Rybarczyk, P. Owczarek, A. Milecki, and P. Bun, "Use of Delta Robot as an Active Touch Device in Immersive Case Scenarios". Procedia Computer Science, Vol. 104, No. 2017, pp. 485-492.

[8] I. Bonev, "Delta parallel robot—the story of success," in *Newsletter, available at http://www.parallelmic.org*, ed, 2001.

[9] M. Ramírez-Neria, H. Sira-Ramírez, A. Luviano-Juárez, and A. Rodrguez-Ángeles, "Active disturbance rejection control applied to a delta parallel robot in trajectory tracking tasks". Asian Journal of Control, Vol. 17, No. 2, 2015, pp. 636-647.

[10] A. Zidan, D. Kaczor, S. Tappe, and T. Ortmaier, "Optimization of a P/PI Cascade Motion Controller for a 3-DOF Delta Robot," in *Tagungsband des 4. Kongresses Montage Handhabung Industrieroboter*, ed: Springer, 2019, pp. 217-226.

[11] L. Angel, J. Sebastian, R. Saltaren, and R. Aracil. "RoboTenis system part II: Dynamics and control". Proceedings of the 44th IEEE Conference on Decision and Control, 2005.

[12] J. Fabian, C. Monterrey, and R. Canahuire. "Trajectory tracking control of a 3 DOF delta robot: a PD and LQR comparison". IEEE International Congress on Electronics, Electrical Engineering and Computing, 2016.

[13] A. Dumlu and K. Erenturk, "Trajectory tracking control for a 3-dof parallel manipulator using fractional-order PI^lambda {D}^mu control". IEEE Transactions on Industrial Electronics, Vol. 61, No. 7, 2013, pp. 3417-3426.

[14] Y.-L. Kuo and P.-Y. Huang, "Experimental and simulation studies of motion control of a Delta robot using a model-based approach". International Journal of Advanced Robotic Systems, Vol. 14, No. 6, 2017, pp. 1-14.

[15] K. P. Jankowski and H. Van Brussel, "An approach to discrete inverse dynamics control of flexible-joint robots". IEEE Transactions on Robotics and Automation, Vol. 8, No. 5, 1992, pp. 651-658.

[16] Y. Su, D. Sun, L. Ren, and J. K. Mills, "Integration of saturated PI synchronous control and PD feedback for control of parallel manipulators". IEEE Transactions on Robotics, Vol. 22, No. 1, 2006, pp. 202-207.

[17] H.-H. Lin, Y.-H. Ta, and C.-S. Liu. "The implementation of smoothing robust control for a delta robot". Second International Conference on Robot, Vision and Signal Processing, 2013.

[18] R. H. Hensen, M. Van de Molengraft, and M. Steinbuch, "Friction induced hunting limit cycles: A comparison between the LuGre and switch friction model". Automatica, Vol. 39, No. 12, 2003, pp. 2131-2137.

[19] H. Olsson and K. J. Astrom, "Friction generated limit cycles". IEEE Transactions on Control Systems Technology, Vol. 9, No. 4, 2001, pp. 629-636.

[20] B. Armstrong-Hélouvry, P. Dupont, and C. C. De Wit, "A survey of models, analysis tools and compensation methods for the control of machines with friction". Automatica, Vol. 30, No. 7, 1994, pp. 1083-1138.

[21] R. H. A. Hellsen, G. Z. Angelis, M. J. G. van de Molengraft, A. G. de Jager, and J. J. Kok, "Grey-box Modeling of Friction: An Experimental Case-study". European Journal of Control, Vol. 6, No. 3, 2000, pp. 258-267.

[22] V. Lampaert, J. Swevers, and F. Al-Bender, "Modification of the Leuven integrated friction model structure". IEEE Transactions on Automatic Control, Vol. 47, No. 4, 2002, pp. 683-687.

[23] C. Makkar, W. E. Dixon, W. G. Sawyer, and G. Hu. "A new continuously differentiable friction model for control systems design". IEEE/ASME International Conference on Advanced Intelligent Mechatronics, Monterey, CA, 2005.

[24] G. Morel, K. Iagnemma, and S. Dubowsky, "The precise control of manipulators with high joint-friction using base force/torque sensing". Automatica, Vol. 36, No. 7, 2000, pp. 931-941.

[25] B. Bona and M. Indri. "Friction Compensation in Robotics: an Overview". IEEE European Control Conference on Decision and Control, Seville, Spain, 2005.

[26] I. Hashlamon and K. Erbatur, "Reduced Filtered Dynamic Model for Joint Friction Estimation of Walking Bipeds". Jordan Journal of Mechanical & Industrial Engineering, Vol. 11, No. 3, 2017,

[27] I. Hashlamon and K. Erbatur, "Joint friction estimation for walking bipeds". Robotica, Vol. 34, No. 7, 2014, pp. 1610-1629.

[28] I. F. Hashlamon, "Joint friction estimation and slip prediction of biped walking robots," PhD diss, Sabanci University, 2014.

[29] A. Mohammadi, M. Tavakoli, H. J. Marquez, and F. Hashemzadeh, "Nonlinear disturbance observer design for robotic manipulators". Control Engineering Practice, Vol. 21, No. 3, 2013, pp. 253-267.

[30] C. Wen-Hua, D. J. Ballance, P. J. Gawthrop, and J. O'Reilly, "A nonlinear disturbance observer for robotic manipulators". IEEE Transactions on Industrial Electronics, Vol. 47, No. 4, 2000, pp. 932-938.

[31] A. Radke and Z. Gao. "A survey of state and disturbance observers for practitioners". American Control Conference, 2006.

[32] H. Sussmann and P. Kokotovic, "The peaking phenomenon and the global stabilization of nonlinear systems". IEEE Transactions on automatic control, Vol. 36, No. 4, 1991, pp. 424-440.

[33] A. A. Ball and H. K. Khalil. "High-gain observers in the presence of measurement noise: A nonlinear gain approach". 2008 47th IEEE Conference on Decision and Control, 2008.

[34] L. A. Castañeda, A. Luviano-Juárez, and I. Chairez, "Robust trajectory tracking of a delta robot through adaptive active disturbance rejection control". IEEE Transactions on Control Systems Technology, Vol. 23, No. 4, 2015, pp. 1387-1398.

[35] H. Wang, "Adaptive Control of Robot Manipulators With Uncertain Kinematics and Dynamics". IEEE Transactions on Automatic Control, Vol. 62, No. 2, 2017, pp. 948-954.

[36] B. Xiao and S. Yin, "Exponential tracking control of robotic manipulators with uncertain dynamics and kinematics". IEEE Transactions on Industrial Informatics, Vol. 15, No. 2, 2018, pp. 689-698.

[37] C. E. Boudjedir, D. Boukhetala, and M. Bouri, "Nonlinear PD plus sliding mode control with application to a parallel delta robot". Journal of Electrical Engineering, Vol. 69, No. 5, 2018, pp. 329-336.

[38] C. Lu, X. Miao, S. Wang, and C. Zhang. "Research on Adaptive Robust Control Algorithm for Delta Parallel Robots". Transactions on Intelligent Welding Manufacturing, Singapore, 2019.

[39] R. Hayat, M. Leibold, and M. Buss, "Robust-Adaptive Controller Design for Robot Manipulators Using the H_infinity Approach". IEEE Access, Vol. 6, No. 2018, pp. 51626-51639.

[40] I. Hashlamon, "A New Adaptive Extended Kalman Filter for a Class of Nonlinear Systems". Journal of Applied and Computational Mechanics, Vol. 6, No. 1 2020, pp. 1-12.

[41] I. Hashlamon and K. Erbatur, "An improved real-time adaptive Kalman filter with recursive noise covariance updating rules". Turkish journal of electrical engineering & computer sciences, Vol. 24, No. 2, 2016, pp. 524-540.

[42] A. Olsson, "Modeling and control of a Delta-3 robot," Master Department of Automatic Control, Lund University, 2009.

[43] P. Hsu, M. Bodson, S. Sastry, and B. Paden. "Adaptive identification and control for manipulators without using joint accelerations". Proceedings IEEE International Conference on Robotics and Automation, Raleigh, NC, USA, 1987.

[44] M. Van Damme, P. Beyl, B. Vanderborght, V. Grosu, R. Van Ham, I. Vanderniepen*, et al.* "Estimating robot end-effector force from noisy actuator torque measurements". IEEE International Conference on Robotics and Automation (ICRA), Shanghai, 2011.

[45] R. Lazzari, "Sensorless Haptic Force Feedback for Telemanipulation using two identical Delta Robots," Master, Automation Engineering, Padova university, 2017.